

Influence of heating conditions on the formation of sol–gel derived calcium hydroxyapatite

Irma Bogdanovičienė¹,

Aldona Beganskienė¹,

Aivaras Kareiva^{1*},

Remigijus Juškėnas²,

Algirdas Selskis²,

Rimantas Ramanauskas²

Kaia Tõnsuaadu³,

Valdek Mikli³

¹ *Department of General and Inorganic Chemistry,
Vilnius University, Naugarduko 24,
LT-03225 Vilnius, Lithuania*

² *Institute of Chemistry of
Center for Physical Sciences and Technology,
A. Goštauto 9, LT-01108 Vilnius, Lithuania*

³ *Laboratory of Inorganic Materials,
Centre for Materials Research,
Tallinn University of Technology,
Ehitajate tee 5, 19086 Tallinn, Estonia*

Calcium hydroxyapatite ($\text{Ca}_{10}(\text{PO}_4)_6(\text{OH})_2$, HA) was obtained in the sol–gel process of an aqueous solution of trans-1,2-diaminocyclohexanetetraacetic acid monohydrate (DCTA) and calcination of precursor gels at 1 000 °C. Aqueous sol–gel chemistry route based on ammonium–hydrogen phosphate as a source of phosphorus and calcium acetate monohydrate as a source of calcium ions have been developed to prepare Ca–P–O gel samples. It has been shown that adjustment of heating time and atmosphere composition can be used to control the synthesis, phase purity and morphology of ceramic samples. Phase transformations, composition and micro-structural features in polycrystalline samples were studied by thermal analysis (TG / DTA), infrared spectroscopy (IR), X-ray powder diffraction analysis (XRD) and scanning electron microscopy (SEM).

Key words: calcium hydroxyapatite, HA, aqueous sol–gel process, DCTA

INTRODUCTION

Calcium hydroxyapatite, $\text{Ca}_{10}(\text{PO}_4)_6(\text{OH})_2$, commonly referred to as HA, is one of the calcium phosphate based bioceramic materials, which makes up the majority of inorganic components in human bones and teeth. Synthetic HA is known to be one of the most important implantable materials due to its biocompatibility, bioactivity and osteoconductivity coming from the analogy to the mineral components of natural bones. The bioactive properties of this compound have shown to provide a faster fixation of implants used in ortho-

pedics (joint replacement implants) and dentistry (endoosseous dental implants). For the use in medical practice, HA ceramics has been conventionally strengthened and toughened in the form of granules and dense or porous ceramic composites, coatings, whiskers, nanorods and different pieces of a complex shape. Although these materials can closely replicate the structure of human bone, improvement of the properties of these materials is still greatly desirable [1–15]. The specific chemical structural and morphological properties of HA bioceramics are highly sensitive, however, to changes in chemical composition and processing conditions [16–19].

A number of papers have been published on different methodologies of the preparation and processing of HA bioce-

* Corresponding author. E-mail: aivaras.kareiva@chf.vu.lt

ramics during the last decade [20]. The solid-state synthesis of HA from oxide or inorganic salt powders usually requires extensive mechanical mixing and lengthy heat treatments at high temperatures [21, 22]. These processing conditions, however, do not allow facile control over micro-structure, grain size and grain size distribution in the resulting powders or shapes. Several wet-chemical and / or soft chemistry techniques, such as polymerized complex routes [23–25], hydrothermal syntheses [26–28], precipitation methods [29–34] or spray-, gel-pyrolysis methods [35, 36] have been used to produce HA phases. Most of these methods suffer from the complex procedures and / or mismatch in the solution behaviour of the constituents. As a consequence, inhomogeneity may be present in the obtained ceramics; e. g., a significant amount of impurity phases are forming. It has been well demonstrated that the sol-gel process offers considerable advantages of a good mixing of the starting materials and an excellent chemical homogeneity and stoichiometry of the product [37–45]. Several sol-gel approaches, starting from nonaqueous solutions of different calcium and phosphorus precursors, have been used for the preparation of HA powders [46–58]. The major limitation for its applications was found to be a very low solubility of calcium alkoxides in organic solvents and their low reactivity which caused deviations from the stoichiometry of the final materials.

The aqueous route of sol-gel preparation offers an effective and relatively simple way to produce HA. Recently, aqueous sol-gel chemistry routes have been developed to prepare calcium hydroxyapatite samples with different morphological properties [59], using ethylenediaminetetraacetic acid (EDTA) or tartaric acid (TA) as complexing agents. $\text{Ca}_{10}(\text{PO}_4)_6(\text{OH})_2$ was obtained by calcination of precursor gels for 5 h at 1 000 °C. Moreover, it has been clearly demonstrated that the phase purity of calcium hydroxyapatite ceramics depends on the gelation temperature used in the sol-gel processing [60]. These results have initiated the present work, motivating us to continue our earlier investigations. In this study, the influence of heating conditions on the formation of HA ceramics was investigated. The Ca–P–O precursor gels were heated up to 1 000 °C in air, O_2 and N_2 atmospheres. Secondly, the calcined gels were also annealed at 1 000 °C for different time in air or water vapour atmospheres. The results are presented herein.

EXPERIMENTAL

In the sol-gel process, calcium acetate monohydrate, $\text{Ca}(\text{CH}_3\text{COO})_2 \cdot \text{H}_2\text{O}$, and ammonium-hydrogen phosphate, $(\text{NH}_4)_2\text{HPO}_4$, were selected as Ca and P sources, respectively, in the Ca / P mole ratio of 1.67. In the first step, calcium acetate monohydrate (5.285 g; 0.03 mol) was dissolved in distilled water under continuous stirring at 65 °C. In order to obtain water-soluble calcium complexes and thereby avoid undesirable crystallization of calcium phosphates, trans-1,2-diaminocyclohexanetetraacetic acid monohydrate (DCTA,

$\text{C}_{14}\text{H}_{22}\text{N}_2\text{O}_8 \cdot \text{H}_2\text{O}$) (11.2 g; 0.03 mol) was dissolved in distilled water and afterwards added to the initial solution. The resulting mixture was stirred for 1 h at the same temperature. Then, $(\text{NH}_4)_2\text{HPO}_4$ (2.376 g; 0.018 mol), dissolved in distilled water, was added to the above-mentioned solution. Finally, after a slow evaporation under continuous stirring at 65 °C, the Ca–P–O sols turned into transparent gels. The oven-dried (100 °C) gel powders were ground in an agate mortar and heated up to 1 000 °C in a tube furnace at the heating rate 10 °C min^{-1} in air, O_2 and N_2 atmospheres and calcined at this temperature for 1–5 h in air and water vapour atmospheres.

The dry gels were characterized by thermal analysis (TG / DTA). The calcination products were investigated by infrared spectroscopy (IR), X-ray powder diffraction (XRD) analysis and scanning electron microscopy (SEM). The thermal analysis was performed using a Setaram TG-DSC12 apparatus in air, O_2 or N_2 flow of 50 ml/min at a heating rate of 10 °C min^{-1} . The IR spectra were recorded as KBr pellets on a Perkin-Elmer FTIR Spectrum BX II spectrometer. The XRD studies were performed on a D8 (Bruker AXS) diffractometer operating with $\text{Cu } K_{\alpha 1}$ radiation (step size: 0.04; time per step: 5 s). In order to study the morphology and microstructure of the ceramic samples, a JEOL JSM 8404 scanning electron microscope was used.

RESULTS AND DISCUSSION

It is well known that temperature control during the synthesis strongly influences the reaction progress and the properties of the resulting HA material [60]. The thermal decomposition of the oven-dried Ca–P–O gels in air, O_2 and N_2 atmospheres was studied by TG / DTA measurements. The TG and DTA curves for the gels are shown in Fig. 1. As one can see, the behaviour of all recorded TG curves differs significantly. The weight measurements carried out in air flow (Fig. 1a) show four main steps in the temperature ranges of 20–196 °C (~6.7%), 196–430 °C (~58.0%), 430–633 °C (~14.5%) and 633–754 °C (~5.5%). The weight loss below 200 °C is due to the evaporation of absorbed and/or structurally incorporated water [16]. The next three significant decomposition steps can be attributed to the pyrolysis of organic constituents, to the removal of acetate and ammonia from the gels, and to the degradation of intermediate species formed during the gelation process [16]. The overall weight loss during the heating of the gel sample up to 770 °C was approximately 84%. The TG curve in the oxygen flow is shown in Fig. 1b. One can see that here are also four main weight losses, but their intensity and temperature range are different from the previous results. The temperature ranges and the weight losses are 20–196 °C (~7.7%), 196–250 °C (~46.3%), 250–516 °C (~24.1%) and 516–758 °C (~8.0%). The overall weight loss determined at 800 °C was approximately 86%. However, quite a different thermogravimetric behaviour was observed when the Ca–P–O gel was heated in the nitrogen atmosphere. The TG curve of these measurements is presented in Fig. 1c. In

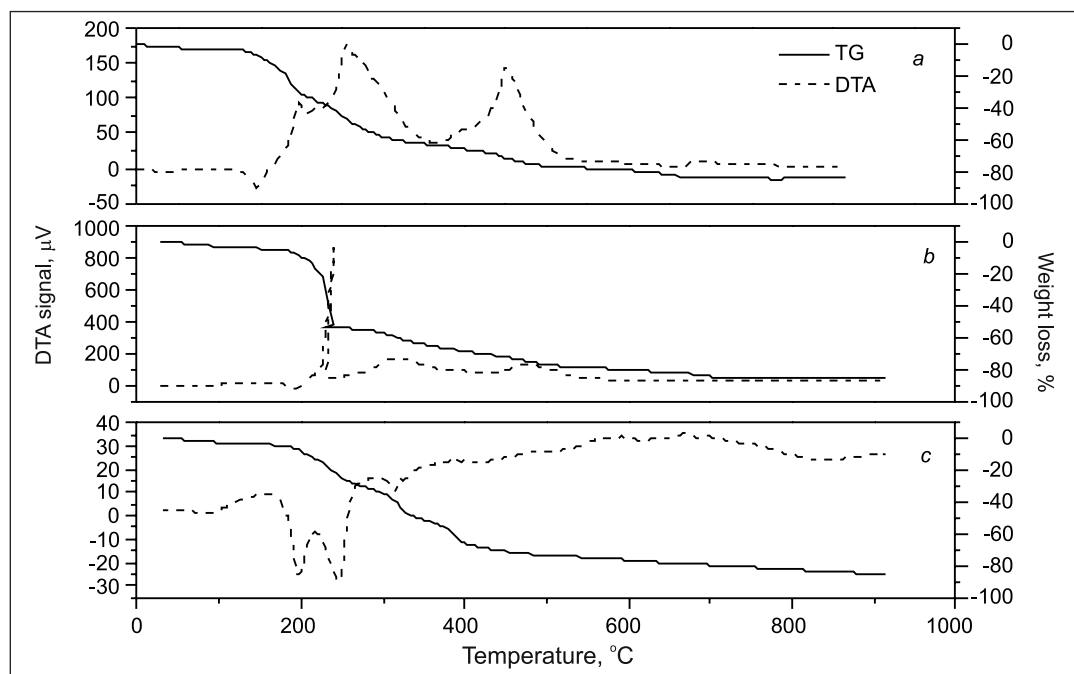


Fig. 1. TG and DTA curves for Ca-P-O precursor gels heated in different atmospheres: *a* – air, *b* – oxygen, *c* – nitrogen

this case, the weight decreased monotonically in the whole temperature interval (20–1000 °C). However, six hardly distinguishable temperature ranges could be also differentiated: 20–160 °C (~3.7%), 160–250 °C (~20.8%), 250–360 °C (~28.5%), 360–520 °C (~21.1%), 520–650 °C (~4.0%), and 650–1000 °C (~7.7%). The overall weight loss determined at 1000 °C was approximately 85%. Thus, at heating Ca-P-O gels in air or oxygen atmosphere, the weight becomes apparently stable at 760 °C. On the other hand, the weight was not steady in the whole temperature range when the experiment was performed in the nitrogen atmosphere.

The DTA curves recorded for Ca-P-O gels in air or oxygen atmospheres were also similar (see Figs. 2*a, b*). The first decomposition step is indicated by broad endothermic peaks at 174–212 °C on the DTA curves. It is assignable to removal of absorbed and chemisorbed water. Exothermic peaks in air at ~246, ~340, ~500 °C and in oxygen at ~240, ~312, ~479 °C, respectively, originate from the decomposition and oxidation processes. Weak and broad endothermic effects in both DTA curves at ~720 °C, corresponding to the mass loss at about ~4% and ~2%, might be associated with the solid state reactions of the $\text{Ca}_{10}(\text{PO}_4)_6(\text{OH})_2$ phase formation [61]. Only the endothermic effects could be seen in the DTA curve at heating the gel in the nitrogen atmosphere (Fig. 1*c*). The explanation of such thermal behaviour, however, is problematic.

The impact of the calcination atmosphere on apatite formation was also followed in the IR spectra of the products heated up to 1000 °C (Fig. 2). The FTIR spectra for the Ca-P-O gel samples annealed in air or oxygen flow were similar, indicating phosphate formation. On the contrary, the FTIR spectrum for the sample annealed in nitrogen flow did not

contain characteristic P-O peaks, or the intensity of some of these peaks was exceptionally low. Consequently, we can easily conclude that the formation of HA phase in nitrogen atmosphere does not proceed.

Previously [62], it has been mentioned that calcium hydroxyapatite formation using a solid state synthesis approach is promoted by H_2O molecules present in the precursor. Therefore, we decided to continue our experimental investigations by heating the Ca-P-O precursor gel in water vapour flow at 1000 °C. The obtained results were compared with those obtained by heating gels in the air.

The IR spectra of Ca-P-O gel samples heated at 1000 °C in an air flow and in a flow of water vapour are shown in Figs. 3 and 4, respectively. The IR spectra of heating products in air or water vapour atmosphere during 1 h were similar, but after 2 h the differences became visible, and after 5 h they were remarkable. In the spectra of heating products of the gel during 1 h at 1000 °C an intensive peak at 3645 cm^{-1} , characteristic of OH stretching vibration in the $\text{Ca}(\text{OH})_2$ structure, is visible. The intensive absorption in the interval from 1218 to 1169 cm^{-1} , the peaks at $730\text{--}733\text{ cm}^{-1}$ and 528 cm^{-1} could be assigned to calcium polyphosphates ($\beta\text{-Ca}_2\text{P}_2\text{O}_7$) [63]. The less intensive absorption bands in the intervals $1430\text{--}1510$, $2360\text{--}3000$, and $3500\text{--}3600\text{ cm}^{-1}$ could be assigned to non-decomposed organic complexes, and peaks at 970 , $610\text{--}613$, and $555\text{--}575\text{ cm}^{-1}$ to $\text{Ca}_3(\text{PO}_4)_2$ [63]. During long-range heating, the intensity of peaks at 3645 , $1430\text{--}1510$, $730\text{--}733$ and 528 cm^{-1} decreased. This is more remarkable in the spectra of products heated in the water vapour atmosphere. In the spectra of samples heated in the water vapour atmosphere, the peak at $3574\text{--}3578\text{ cm}^{-1}$, assigned to OH vibration in HA structure, increased in prolonged time, and peaks at $630\text{--}632$

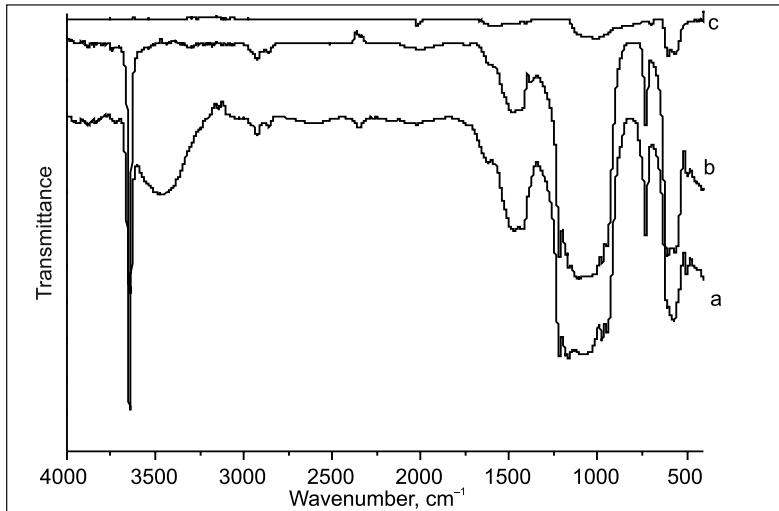


Fig. 2. FTIR spectra for Ca-P-O precursor gels heated up to 1000 °C in different atmospheres: a – air, b – oxygen, c – nitrogen

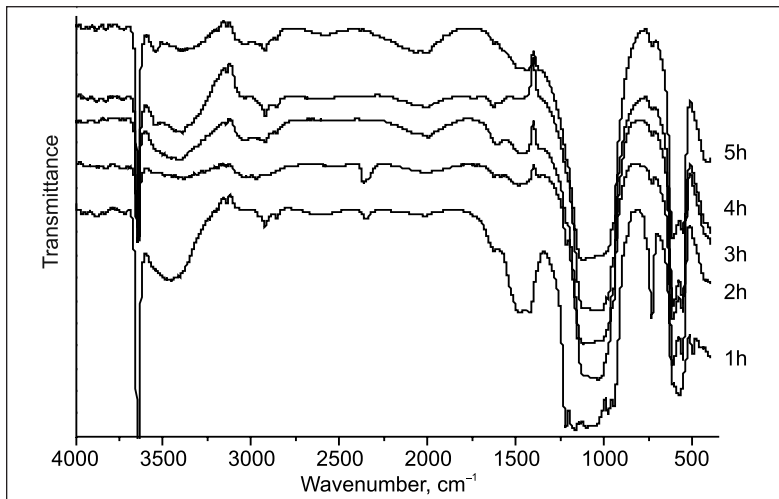


Fig. 3. FTIR spectra of HA samples synthesized at 1000 °C in flowing air atmosphere at different duration of annealing

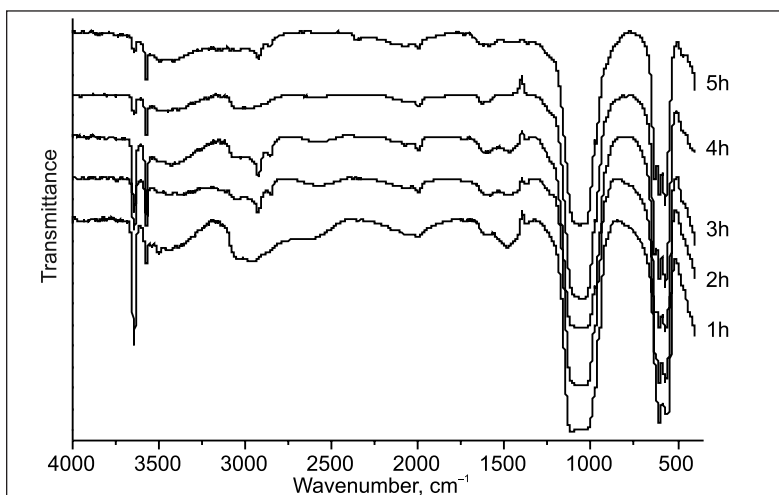


Fig. 4. FTIR spectra of HA samples synthesized at 1000 °C in water vapour flow at different duration of annealing

and 476 cm^{-1} , characteristic of the crystalline HA spectrum, appeared [64]. In a dry air flow, these changes are almost invisible. Therefore, water vapour contributes to and accelerates the formation of HA from Ca-P-O gels under calcination.

The XRD patterns of HA ceramic samples after calcination of Ca-P-O precursor gels in different atmospheres (air or water vapour) for 1–5 h are shown in Figs. 5 and 6. One can see that during calcination of the precursor gel at 1000 °C for 1 h in the air, the product consisted of crystalline and amorphous phases. The most intensive diffraction lines located at $2\theta \approx 28^\circ, 29^\circ, 34^\circ$ could be attributed to the $\beta\text{-Ca}_3(\text{PO}_4)_2$ phase (PDF [9-0169]). With increasing the heating time from 2 to 4 h, low intensity peaks appeared in the range $2\theta \approx 31\text{--}33^\circ$, which are attributable to calcium hydroxyapatite. However, the most intensive peaks remained to be characteristic reflections of $\beta\text{-Ca}_3(\text{PO}_4)_2$ phase. Finally, with the further annealing up to 5 h in the air flow, the $\beta\text{-Ca}_3(\text{PO}_4)_2$ was the main phase in the ceramic product. The XRD analysis has showed that Ca-P-O gels calcined at 1000 °C in water vapour flow for different annealing time are also multiphase materials. Their diffraction patterns are displayed in Fig. 6. However, depending on the heating time, there was an obvious tendency of change in the composition of materials. According to the XRD results, the sample heated for 1 h already had three intensive peaks belonging to the desirable $\text{Ca}_{10}(\text{PO}_4)_6(\text{OH})_2$ phase. Moreover, there was a large number of peaks corresponding to the $\beta\text{-Ca}_3(\text{PO}_4)_2$ phase (PDF [9-0169]). The number and intensity of the calcium phosphate peaks decreased with increasing the heating time. Finally, polycrystalline $\text{Ca}_{10}(\text{PO}_4)_6(\text{OH})_2$ with a small amount of $\beta\text{-Ca}_3(\text{PO}_4)_2$ was obtained after heating for 5 h. The three most intensive lines in the sample were located between $2\theta \sim 31\text{--}33^\circ$ ($(2\ 1\ 1) - 100\%$, $(3\ 0\ 0) - 63.4\%$, and $(1\ 1\ 2) - 52.7\%$) as noted also by other authors [33, 65–67]. These results are also in good agreement with the reference data for $\text{Ca}_{10}(\text{PO}_4)_6(\text{OH})_2$ (PDF

[9–0432]). All accepted $\text{Ca}_{10}(\text{PO}_4)_6(\text{OH})_2$ reflections from our XRD measurements were indexed. The lattice parameters of the synthesized $\text{Ca}_{10}(\text{PO}_4)_6(\text{OH})_2$ sample were obtained from the diffraction pattern by fitting the peaks of identified reflections. The hexagonal lattice parameters and cell volume of the gel heated for 5 h at 1 000 °C in a water vapour flow was found to be $a = 9.42(3)$ and $c = 6.89(2)$. The refined lattice parameters of the HA samples were in good agreement with those reported in [34, 68] with only a small deviation. So, it is obvious that annealing in flow of water vapour promotes the formation of calcium hydroxyapatite considerably.

Calcined Ca–P–O gel precursor powders were investigated by scanning electron microscopy, from which the grain size and typical morphologies of HA could be observed. The morphological features of the ceramic samples heated in air and water vapour flows are presented in the SEM pictures (see Figs. 7–9). Figure 7 shows the SEM micrograph of Ca–P–O gel powders heated in the air atmosphere for 5 h. One can see that the product is composed of different size and shape agglomerated particles. The predominant plate-like crystallites 1–3 μm in size could be assigned to the $\text{Ca}_3(\text{PO}_4)_2$ phase. During heating in a water vapour flow (see Figs. 8, 9), more

Fig. 5. X-ray diffraction patterns of HA samples synthesized at 1 000 °C in flowing air atmosphere at different duration of annealing (TCP – $\beta\text{-Ca}_3(\text{PO}_4)_2$ phase)

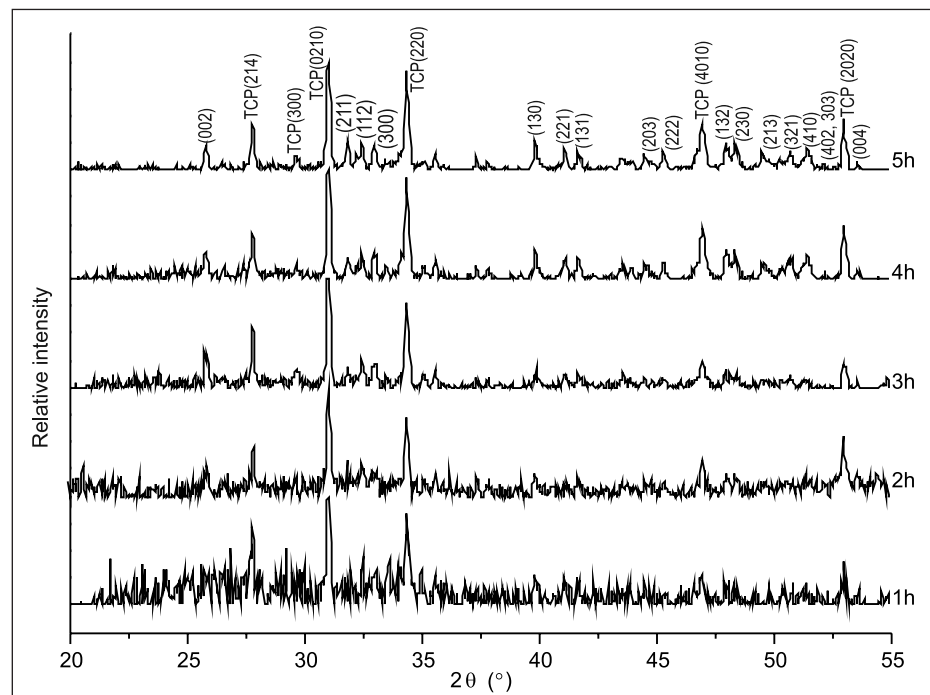
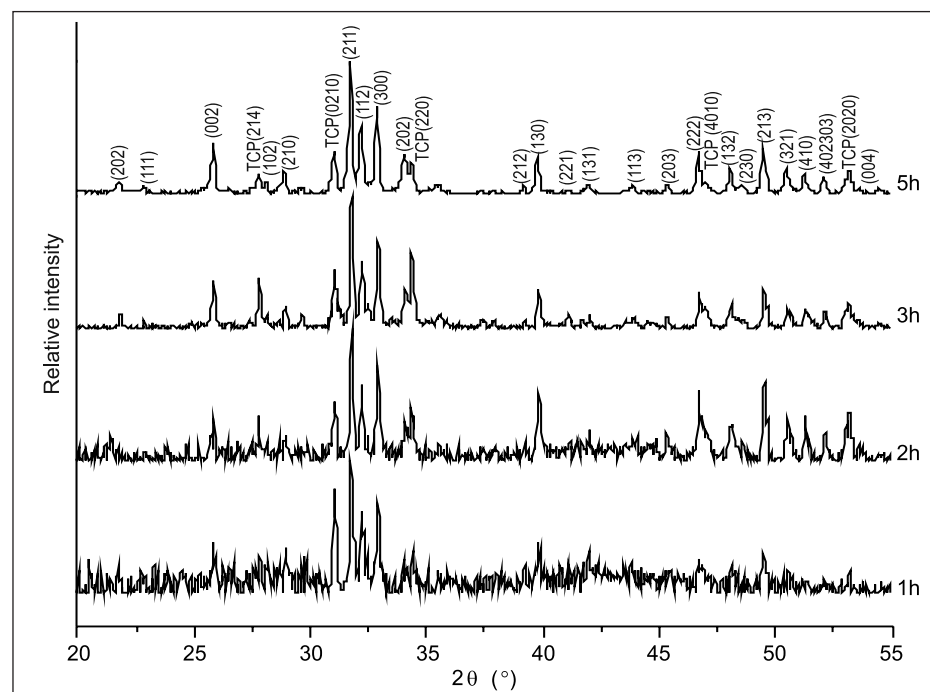


Fig. 6. X-ray diffraction patterns of the HA samples synthesized at 1 000 °C in water vapour flow at different duration of annealing (TCP – $\beta\text{-Ca}_3(\text{PO}_4)_2$ phase)



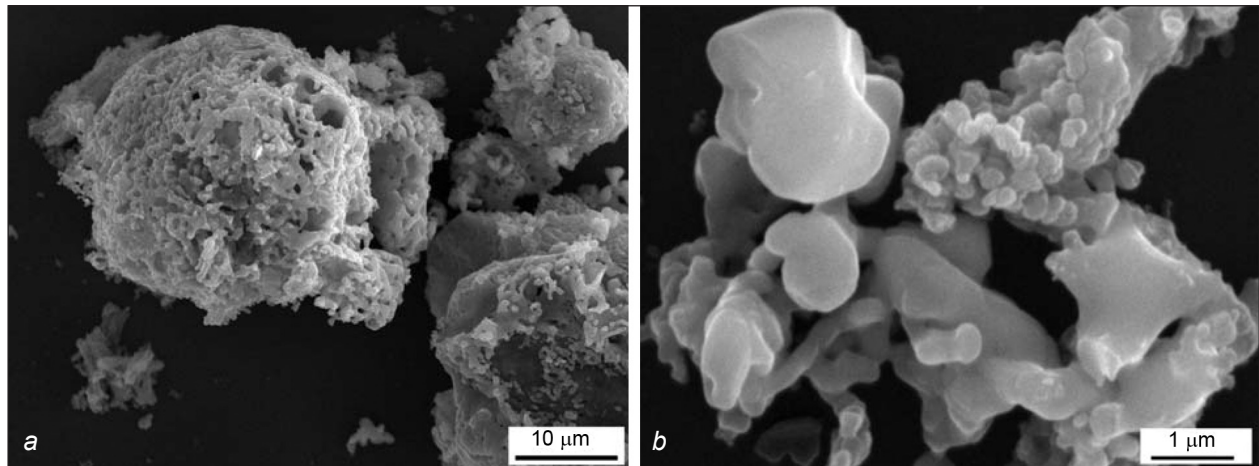


Fig. 7. SEM micrographs of HA samples synthesized at 1000 °C for 5 h in flowing air atmosphere. Magnification: (a) 200x, (b) 2000x

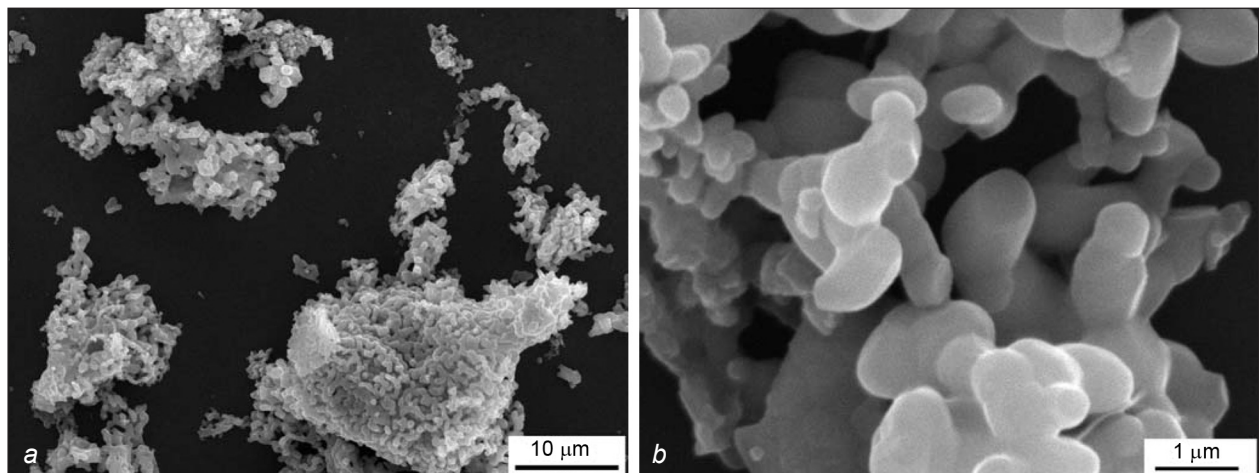


Fig. 8. SEM micrographs of HA samples synthesized at 1000 °C for 1 h in water vapour flow. Magnification: (a) 200x, (b) 2000x

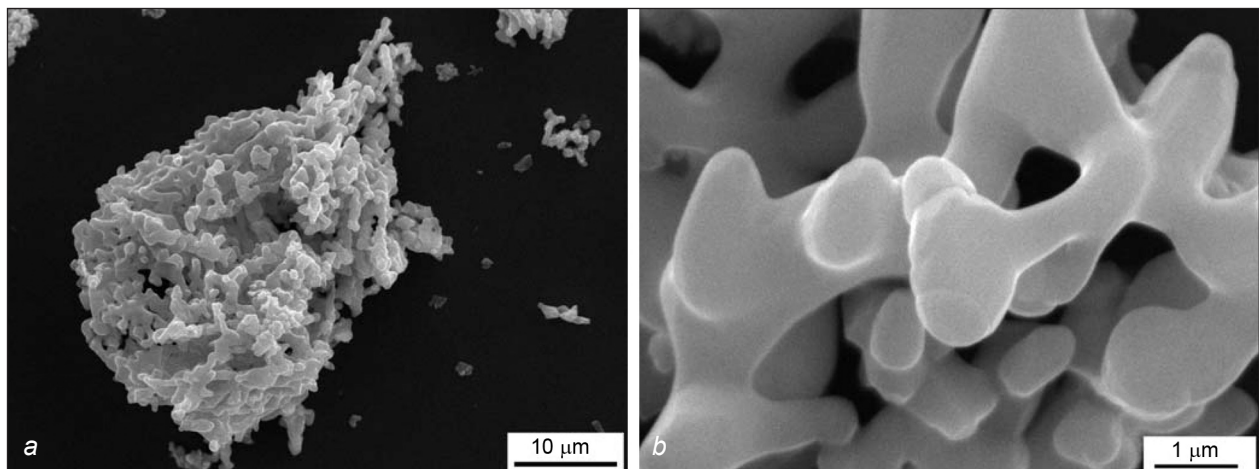


Fig. 9. SEM micrographs of HA samples synthesized at 1000 for 5 h in water vapour flow. Magnification: (a) 200x, (b) 2000x

agglomerated solids were formed. The HA particles obtained after heating for 1 h were composed of agglomerates of interconnected elongated crystallites 0.5 μm wide and 1–1.5 μm long. A small amount of spherical particles (0.2–0.4 μm) were also present on the surface. With increasing the heat-

ing time to 5 h, a SEM micrograph (Fig. 9) showed only large (0.5–2.5 μm) planar crystallites of $\text{Ca}_{10}(\text{PO}_4)_6(\text{OH})_2$ necked to each other. It could be concluded that the annealing conditions have an essential impact on the shape and size of particles in the fusion process of HA bioceramics.

CONCLUSIONS

An aqueous sol-gel chemistry route based on ammonium-hydrogen phosphate and calcium acetate monohydrate as a source of phosphorus and calcium ions, respectively, has been developed to prepare calcium hydroxyapatite (HA). In the sol-gel process, trans-1,2-diaminecyclohexanetetraacetic acid monohydrate (DCTA) was used as a complexing agent. It has been demonstrated that a proper selection of annealing conditions in the high-temperature processing allows to control the phase purity and grain size of the resulting $\text{Ca}_{10}(\text{PO}_4)_6(\text{OH})_2$ powders. It has been concluded, for the first time to our knowledge, that HA formation is considerably promoted by calcinating the precursor gels in a water vapour flow. Also, the purity of HA phase increases with increasing the heating duration. Besides, the morphological properties can be also controlled by changing the annealing atmosphere. Moreover, due to heating the gel in a dry atmosphere, a significant amount of $\text{Ca}_3(\text{PO}_4)_2$ impurities has formed. We have found that HA formation in the nitrogen atmosphere does not take place. In conclusion, the heating of Ca-P-O precursor gels in a water vapour flow allows synthesizing HA ceramic material of a unique crystalline shape.

Received 2 April 2010

Accepted 13 April 2010

References

1. M. Vallet-Regi, *J. Chem. Soc. Dalton. Trans.*, **2**, 97 (2001).
2. L. Hermansson, L. Kraft, H. Engqvist, *Adv. Ceram. Compos. Key. Eng. Mater.*, **247**, 437 (2003).
3. T. Kokubo, H. M. Kim, M. Kawashita, *Biomater.*, **24**, 2161 (2003).
4. L. Gan, J. Wang, A. Tache, N. Valiquette, D. Deporter, R. Pilliar, *Biomater.*, **25**, 5313 (2004).
5. M. Shirkhazadeh, *J. Mater. Sci: Mater. Med.*, **16**, 37 (2005).
6. A. C. Tas, F. Aldinger, *J. Mater. Sci: Mater. Med.*, **16**, 167 (2005).
7. S. C. G. Leeuwenburgh, J. G. C. Wolke, J. Schoonman, J. A. Jansen, *Thin Solid Films*, **472**, 105 (2005).
8. A. H. Choi, B. Ben-Nissan, *Nanomedicine*, **2**, 51 (2007).
9. A. Y. P. Mateus, C. C. Barrias, C. Ribeiro, M. P. Ferraz, F. J. Monteiro, *J. Biomed. Mater. Res. Part A*, **2**, 483 (2008).
10. M. S. Djosic, V. B. Miskovic-Stankovic, S. Milonjic, Z. M. Kacarevic-Popovic, N. Bibic, J. Stojanovic, *Mater. Chem. Phys.*, **111**, 137 (2008).
11. T. F. Stoica, C. Morosanu, A. Slav, T. Stoica, P. Osiceanu, C. Anastasescu, M. Gartner, A. Zaharescu, *Thin Solid Films*, **516**, 8112 (2008).
12. K. Madhumathi, N. S. Binulal, H. Nagahama, H. Tamura, K. T. Shalumon, N. Selvamurugan, S. V. Nair, R. Jayakumar, *Int. J. Biol. Macromol.*, **44**, 1 (2009).
13. N. Matsumoto, K. Yoshida, K. Hashimoto, Y. Toda, *J. Ceram. Soc. Jpn.*, **117**, 249 (2009).
14. H. Wang, C. Z. Chen, D. G. Wang, *Surf. Eng.*, **25**, 131 (2009).
15. H. Khireddine, S. Saoudi, S. Ziani, S. Meski, S. Meskour, *Asian J. Chem.*, **21**, 3885 (2009).
16. A. Bigi, E. Boanini, K. Rubini, *J. Solid. State Chem.*, **177**, 3092 (2004).
17. J. Liu, K. Li, H. Wang, M. Zhu, H. Yan, *Chem. Phys. Lett.*, **396**, 429 (2004).
18. C. E. Fowler, M. Li, S. Mann, H. C. Margolis, *J. Mater. Chem.*, **15**, 3317 (2005).
19. G. Goller, F. N. Oktar, S. Agathopoulos, D. U. Tulyaganov, J. M. F. Ferreira, E. S. Kayali, I. Peker, *J. Sol-Gel Sci. Technol.*, **37**, 111 (2006).
20. S. V. Dorozhkin, *J. Mater. Sci.*, **44**, 2343 (2009).
21. G. De With, H. J. A. Van Dijk, N. Hattu, K. Puijs, *J. Mater. Sci.*, **16**, 1592 (1981).
22. A. Bigi, S. Panzavolta, K. Rubini, *Chem. Mater.*, **16**, 3740 (2004).
23. M. Aizawa, T. Hanazawa, K. Itatani, F. S. Howell, A. Kishio-ka, *J. Mater. Sci.*, **34**, 2865 (1999).
24. H. K. Varma, S. N. Kalkura, R. Sivakumar, *Ceram. Int.*, **24**, 467 (1998).
25. M. Iijima, J. Moradian-Oldak, *Biomaterials*, **26**, 1595 (2005).
26. M. Yoshimura, H. Suda, K. Okamoto, K. Ioku, *J. Mater. Sci.*, **29**, 3399 (1994).
27. D. Janackovic, I. Jankovic, R. Petrovic, L. Kostic-Gvozdenovic, S. Milonjic, D. Uskokovic, *Key Eng. Mater.*, **240-242**, 437 (2003).
28. J. B. Liu, X. Y. Ye, H. Wang, M. K. Zhu, B. Wang, H. Yan, *Ceram. Int.*, **29**, 629 (2003).
29. A. Slosarczyk, E. Stobierska, Z. Paszkiewicz, M. Gawlicki, *J. Am. Ceram. Soc.*, **79**, 2539 (1996).
30. H. Kandori, N. Horigami, A. Yasukawa, *J. Am. Ceram. Soc.*, **80**, 1157 (1997).
31. A. Lopez-Macipe, J. Gomez-Morales, R. Rodriguez-Clemente, *Adv. Mater.*, **10**, 49 (1998).
32. R. N. Panda, M. F. Hsieh, R. J. Chung, T. S. Chin, *J. Phys. Chem. Solids*, **64**, 193 (2003).
33. M. Kawata, H. Uchida, K. Itatani, I. Okada, S. Koda, M. Aizawa, *J. Mater. Sci. Mater. Med.*, **15**, 817 (2004).
34. H. V. Kim, Y. H. Koh, Y. M. Kong, J. G. Kang, H. E. Kim, *J. Mater. Sci. Mater. Med.*, **15**, 1129 (2004).
35. A. Osaka, K. Tsuru, H. Iida, C. Ohtsuki, S. Hayakawa, Y. Miura, *J. Sol-Gel Sci. Technol.*, **8**, 655 (1997).
36. H. K. Varma, S. S. Babu, *Ceram. Int.*, **31**, 109 (2005).
37. C. J. Brinker, G. W. Scherrer, *Sol-Gel Science: The Physics and Chemistry of Sol-Gel Processing*, Academic Press, San Diego (1990).
38. J. Livage, P. Barboux, F. Taulelle, *J. Non-Cryst. Solids*, **147-148**, 18 (1992).
39. J. Zarzycki, *J. Sol-Gel Sci. Technol.*, **8**, 17 (1997).
40. D. R. Uhlmann, G. J. Teowee, *J. Sol-Gel Sci. Technol.*, **13**, 153 (1998).
41. C. Sanchez, F. Ribot, B. Lebeau, *J. Mater. Chem.*, **9**, 35 (1999).
42. C. Sanchez, B. Lebeau, F. Ribot, *J. Sol-Gel Sci. Technol.*, **19**, 31 (2000).

43. A. Baranauskas, D. Jasaitis, A. Kareiva, *Vibr. Spectrosc.*, **28**, 263 (2002).
44. C. Sanchez, G. J. D. A. A. Soler-Illia, F. Ribot, D. Grosso, *CR Chimie*, **6**, 1131 (2003).
45. B. L. Cushing, V. L. Kolesnichenko, C. J. O'Connor, *Chem. Rev.*, **104**, 3893 (2004).
46. Y. Masuda, K. Matubara, S. Sakka, *J. Ceram. Soc. Jpn.*, **98**, 1255 (1990).
47. P. Layrolle, A. Lebugle, *Chem. Mater.*, **6**, 1996 (1994).
48. A. Jillavenkatesa, Sr. R. A. Condrate, *J. Mater. Sci.*, **33**, 4111 (1998).
49. W. J. Weng, J. L. Baptista, *Biomaterials*, **19**, 125 (1998).
50. P. Layrolle, A. Ito, T. Tateishi, *J. Am. Ceram. Soc.*, **81**, 1421 (1998).
51. C. S. Chai, K. A. Gross, B. Ben-Nissan, *Biomaterials*, **19**, 2291 (1998).
52. B. Ben-Nissan, D. D. Green, G. S. K. Kannangara, C. S. Chai, A. Milev, *J. Sol-Gel Sci. Technol.*, **21**, 27 (2001).
53. D. M. Liu, T. Troczynski, W. J. Tseng, *Biomaterials*, **22**, 1721 (2001).
54. M. F. Hsieh, L. H. Perng, T. S. Chin, H. G. Perng, *Biomaterials*, **22**, 2601 (2001).
55. E. Tkalcec, M. Sauer, R. Nonninger, H. Schmidt, *J. Mater. Sci.*, **36**, 5253 (2001).
56. S. R. Ramanan, R. Venkatesh, *Mater. Lett.*, **58**, 3320 (2004).
57. H. Zreiqat, R. Roest, S. Valenzuela, A. Milev, B. Ben-Nissan, *Key Eng. Mater.*, **284–286**, 541 (2005).
58. A. Beganskienė, I. Bogdanovičienė, A. Kareiva, *Chemija*, **2–3**, 16 (2006).
59. I. Bogdanovičienė, A. Beganskiene, K. Tönsuaadu, J. Glaser, H. J. Meyer, A. Kareiva, *Mater. Res. Bull.*, **41**, 1754 (2006).
60. I. Bogdanovičienė, K. Tönsuaadu, A. Kareiva, *Polish J. Chem.*, **83**, 47 (2009).
61. K. Tönsuaadu, M. Peld, V. Bender, *J. Therm. Anal. Calorim.*, **72**, 363 (2003).
62. W. Kim, Q. W. Zhang, F. Saito, *J. Mater. Sci.*, **35**, 5401 (2000).
63. R. A. Nyquist, C. L. Putzig, M. A. Leugers, *Infrared and Raman Spectral Atlas of Inorganic Compounds and Organic Salts: Text and Explanations*. Academic Press, San Diego (1996).
64. A. Antonakos, E. Liarokapis, T. Leventouri, *Biomater.*, **28**, 3043 (2007).
65. M. Manso-Silvan, M. Langlet, C. Jimenez, M. Fernandez, J. M. Martinez-Duart, *J. Eur. Ceram. Soc.*, **23**, 243 (2003).
66. T. M. G. Chu, J. W. Halloran, S. J. Hollister, S. E. Feinberg, *J. Mater. Sci. Mater. Med.*, **12**, 471 (2001).
67. H. Y. Yasuda, S. Mahara, T. Nishiyama, Y. Umakoshi, *Sci. Technol. Adv. Mater.*, **3**, 29 (2002).
68. F. Miyaji, Y. Kono, Y. Suyama, *Mater. Res. Bull.*, **40**, 209 (2005).

Irma Bogdanovičienė, Aldona Beganskienė, Aivaras Kareiva, Remigijus Juškėnas, Algirdas Selskis, Rimantas Ramanauskas, Kaia Tönsuaadu, Valdek Mikli

KAITINIMO SĄLYGŲ ĮTAKA KALCIO HIDROKSIA-PATITO, SINTETINTO ZOLIŲ–GELIŲ METODU, SUSIDARYMUI

S a n t r a u k a

Vandeniniu zolių–gelių metodu susintetintas Ca–P–O gelis. Šiai sintezei amonio–vandenilio fosfatas ir kalcio acetato monohidratas pasirinkti kalcio ir fosforo šaltiniai, o 1,2-diamincikloheksantetraacto rūgšties monohidratas (DCTA) naudotas kaip kompleksus sudarantis reagentas. Gelio pavyzdžiai buvo kaitinti skirtingą laiką oro, deguonies, azoto ir vandens garų aplinkose, 1000 °C temperatūroje. Kaitinimo metu vykstantys procesai ir gautų junginių sudėtis bei morfologija tirti terminės analizės (TG / DTA), infraraudonųjų spindulių spektroskopijos (IR), Rentgeno spindulių difrakcinės analizės (XRD) bei skenuojančios elektroninės mikroskopijos (SEM) metodais. Nustatyta, kad vandens garų aplinka gelio kaitinimo metu sudaro palankiausias sąlygas kalcio hidroksiapatitui (HA) susidaryti, o gautos keramikos fazinis grynumas ir morfologinės savybės tiesiogiai priklauso nuo kaitinimo laiko. Be to, mūsų žiniomis, HA sintezė vandens garų aplinkoje buvo atlikta pirmą kartą. Po kaitinimo oro aplinkoje gautoje keramikoje susidarė HA ir didelė dalis β -Ca₃(PO₄)₂ priemaišinės fazės, o azoto aplinkoje HA visai nesudarė. Šie rezultatai parodė, kad teisingai pasirinkus kaitinimo sąlygas, galima kontroliuoti gaunamų junginių fazinį grynumą ir kitas savybes. Kaitinant Ca–P–O gelį vandens garų aplinkoje, susintetintas HA keramikos pavyzdys, pasižymintis savitomis morfologinėmis savybėmis.